https://doi.org/10.5194/hess-2020-167
Preprint. Discussion started: 12 May 2020

Hydrology and Earth System Sciences
Discussions

Uncertainty analysis of the rate of change of quantile due to global warming using uncertainty analysis of non-stationary frequency model of peak-over-threshold series

Okjeong Lee

Department of Environmental Engineering, Pukyong National University, Busan 48513 Korea

Jeonghyeon Choi

Division of Earth Environmental System Science, Major of Environmental Engineering, Pukyong National University, Busan 48513 Korea

Jeongeun Won

Division of Earth Environmental System Science, Major of Environmental Engineering, Pukyong National University, Busan 48513 Korea

Sangdan Kim

Corresponding author, Department of Environmental Engineering, Pukyong National University, Busan 48513 Korea. E-mail: skim@pknu.ac.kr

https://doi.org/10.5194/hess-2020-167
Preprint. Discussion started: 12 May 2020

Hydrology and Earth System Sciences
Discussions

Abstract

Several methods have been proposed to analyze the frequency of non-stationary anomalies. The applicability of the non-stationary frequency analysis has been mainly evaluated based on the agreement between the time series data and the applied probability distribution. However, since the parameters of the estimated probability distribution contain a lot of uncertainty, the uncertainty in the correspondence between samples and probability distribution is inevitably large. In this study, an extreme rainfall frequency analysis is performed that fits the Peak-over-threshold series to the covariate-based non-stationary Generalized Pareto distribution. By quantitatively evaluating the uncertainty of daily rainfall quantile estimates at Busan and Seoul sites of the Korea Meteorological Administration using the Bayesian approach, we tried to evaluate the applicability of the non-stationary frequency analysis with a focus on uncertainty. From the point of view of the agreement between the time series data and the applied probability distribution, the non-stationary model was found to be slightly better. When comparing the performance of the stationary and non-stationary model from the uncertainty point of view, the uncertainty of the non-stationary model was greater than that of the stationary model since the non-stationary model included variability arising from covariates. However, it was found that if the appropriate covariate corresponding to the quantile was selected (that is, if the variability of the covariate was eliminated), the reliability of the non-stationary model could be higher than that of the stationary model. Given the covariate, it was confirmed that the uncertainty reduction in quantile estimates for the increase in sample size is more pronounced in the non-stationary model. In addition, how to use the dew point-based non-stationary frequency analysis when integrating information on global temperature rise is described. Finally, it is proposed how to quantify the uncertainty of the rate of change in the future quantile due to global warming using the rainfall quantile ensemble obtained in the uncertainty analysis process.

Keywords: Co-variate, Generalized Pareto distribution, Non-stationary frequency analysis, Peak-over-threshold time series, Uncertainty

https://doi.org/10.5194/hess-2020-167
Preprint. Discussion started: 12 May 2020


Hydrology and Earth System Sciences
Discussions

1. Introduction

Human activity in the last century has caused global surface air temperature to rise (Karl et al., 2009; Min et al., 2011). When the temperature rises by 1 °C, the moisture retention capacity in the atmosphere increases by about 7 %, which directly affects precipitation (Trenberth, 2011; Sim et al., 2019). The higher the water vapor in the atmosphere, the more likely it is to increase precipitation (Berg et al., 2013), and increasing surface air temperature and increasing atmospheric moisture content can increase probable maximum precipitations or rainfall extremes (Kunkel et al., 2013; Lee and Kim, 2018). As a result, global warming damages the performance of drainage system infrastructure such as embankments, sewers and dams (Das et al., 2011; Jongman et al., 2014), increasing the risk of climate extremes (Emori and Brown, 2005; Hao et al., 2013). In fact, looking at ground observations around the world shows that rainfall extremes have increased significantly over the past century (Karl and Knight, 1998; DeGaetano, 2009). Global studies have shown that precipitation has increased in northern Australia, Central Africa, Central America, and Southwest Asia (Groisman et al., 2012).

The current infrastructure design concept for dealing with rainfall extremes is based on the estimation of design rainfall depth using frequency analysis of annual maximum series for various durations in a region (Madsen et al., 2002; Hosking and Wallis, 2005; Sugahara et al ., 2009; Haddad et al., 2011; Willems, 2013; Kim et al., 2020). Current design rainfall depth is based on the concept of stationarity in time, which assumes that the probability of occurrence of extreme rainfall events is not expected to change significantly over time. However, this probability is expected to change due to global warming (Lee et al., 2016), and this change is called non-stationarity in many documents (Alexander et al., 2006; Gregersen et al., 2013).

Several methods have been proposed to deal with time series non-stationarity (Cunha et al., 2011; Yilmaz et al., 2013; Jang et al., 2015, Moon et al., 2016), and many studies on changes in design rainfall depth or its return level under non-stationary conditions have been conducted (Salvadori and DeMichele, 2010; Graler et al., 2013; Hassanzadeh et al., 2013; Salas and Obeysekera, 2013; Shin et al., 2014; Choi et al ., 2019). Looking at the probability distributions and parameters applied to the above studies, most of the non-stationary frequency analysis is performed by expressing specific parameters of the Gumbel or Generalized Extreme Value (GEV) distribution as a function of covariate including time (Kim et al., 2017). In extreme

https://doi.org/10.5194/hess-2020-167
Preprint. Discussion started: 12 May 2020

rainfall series, non-stationarity may be explicitly expressed as a function of time, but may also be related to climate variables in the same or preceding time periods where rainfall extremes occurred (Zhang et al., 2010). Several studies have reported that it is reasonable to use climate variables rather than time for covariates to represent non-stationarities in the non-stationary frequency analysis (Agilan and Umamahesh, 2016; Sen et al., 2020). Recently, studies have been performed that analyze the non-stationary frequency using climate variables for annual maximum rainfall series (Villarini et al., 2012; Agilan and Umamahesh, 2017; Lee et al., 2018; Ouarda et al., 2019). In addition, studies have been conducted to analyze the non-stationary frequency using Peak-over-threshold (POT) series for the purpose of reducing the uncertainty occurring in the sample size (Tramblay et al., 2013; Jung et al., 2018; Lee et al., 2019).

In this research trend, what is of interest in this study is how to examine the relative superiority of the stationary and non-stationary models. Most studies use Akaike Information Criterion (AIC) and similar indicators, which evaluates how well the time series and probability distribution match, to select the optimal model from various candidate non-stationary model, including the stationary model (Akaike, 1974; Ganguli and Coulibaly, 2017; Iliopoulou et al., 2018; Lee et al., 2019). However, the results of selecting the optimal model by these methods are highly likely to vary depending on the sample size. On the other hand, the uncertainty of rainfall quantile as a result of frequency analysis can be an important determinant in the selection of the optimal model. This is because a model with relatively small uncertainty in the estimated rainfall quantile can be regarded as a more reliable model.

Whether or not the non-stationary model provides more reliable rainfall quantile estimates than the stationary model raises a lot of controversy. Serinaldi and Kilsby (2015) warned that uncertainty in non-stationary models might be greater since non-stationary models were more complex than stationary models. Agilan and Umamahesh (2018) investigated the effect of covariate selection on uncertainty in the covariate-based non-stationary analysis using annual maximum series. Ouarda et al. (2020) indicated that uncertainty is likely to work as a major weakness in the applicability of the non-stationary model through the analysis of UAE annual maximum rainfall series.

In this study, a non-stationary frequency analysis using dew-point temperature (DPT) as a covariate is performed. The uncertainty in analyzing the non-stationary frequency of rainfall

https://doi.org/10.5194/hess-2020-167
Preprint. Discussion started: 12 May 2020


Hydrology and Earth System Sciences
Discussions

extremes using the annual maximum series inevitably includes the uncertainty due to the limitation of the sample size. In this study, the POT series is extracted from daily rainfall data with the aim of reducing the uncertainty that comes from sample size as much as possible. Using the Bayesian approach, the parameters of the stationary and non-stationary Generalized Pareto (GP) distributions for the POT excesses are sampled from the posterior distribution. Using this, the performance of the stationary and non-stationary frequency analysis is investigated in terms of uncertainty. We will also examine how uncertainty in the non-stationary frequency analysis can be reduced by determining the appropriate covariate value (i.e., DPT value) corresponding to the rainfall quantile. Finally, the rate of change in rainfall quantile estimates for various DPT rise scenarios considering global warming will be analyzed based on uncertainty analysis.

2. Methods

2.1 Peak-over-threshold series and Generalized Pareto distribution

In this study, daily precipitation and daily DPT data from 1961 to 2017 at the Korea Meteorological Agency's Busan and Seoul sites were used. Figure 1 shows the results of quantile regression using daily precipitation data and DPT data on the day of precipitation observed at Busan and Seoul sites. Daily rainfall depth of 0.1 mm or more was applied to the analysis, and a regression slope of 95 % extreme daily rainfall depth corresponding to DPT was estimated. For reference, the quantile regression equation for the quantile τ (0.95 in Figure 1) given in the quantile regression analysis is as follows:

$$\ln R_\tau = a + bT, \quad (1)$$

where R_τ is the daily rainfall depth, and T is the DPT of the day when the daily rainfall occurred. The following Eq. (2) was constructed using Eq. (1) to see how much the daily rainfall increases or decreases when DPT increases by 1 ℃:

$$\mathrm{d}R_\tau/\mathrm{K} = 100(e^b - 1). \quad (2)$$

From Figure 1, it can be found that when DPT increases by 1 ℃, daily rainfall increases by 7 to 8 %.

https://doi.org/10.5194/hess-2020-167
Preprint. Discussion started: 12 May 2020


Hydrology and Earth System Sciences
Discussions

141

142 [Figure 1. Sensitivity of 95 % daily rainfall depth to dew-point temperature at (a) Busan and
143 (b) Seoul sites.]

144

145 In general, rainfall frequency analysis is performed using the annual maximum series or
146 POT series. In the annual maximum series approach, the annual maximum rainfall series is
147 generally assumed to follow the GEV distribution, and various studies have been conducted
148 (Cheng et al., 2014). However, as the annual maximum series approach only considers one
149 sample per year, the information contained in other data is completely ignored, so the POT
150 approach to select the maximum number of samples for frequency analysis is being studied as
151 an alternative (Hosseinzadehtalaei et al., 2017). In other words, since the POT approach uses
152 more samples to enable accurate parameter estimation of the distribution, several studies
153 recommend using the POT series instead of the annual maximum series (Yilmaz et al.,
154 2014). The POT series is generally assumed to follow the GP distribution (Coles et al., 2001).

155 The cumulative probability distribution function of the stationary GP distribution for the
156 POT series is as follows (Hosking and Wallis, 1987):

157 $$F(x) = 1 - \left(1 - k\frac{x - x_o}{\alpha}\right)^{1/k}, \quad (3)$$

158 where the range of x is $x_o < x < \infty$, α is the scale parameter, and k is the shape parameter
159 ($k < 0$). The threshold x_o should be determined in advance. The random variable x has a
160 value greater than x_o, and it is assumed that the occurrence of x follows the Poisson
161 distribution described by the annual incidence λ. The annual incidence λ can be defined as
162 the number of selected POT excesses divided by the observation year.

163 To ensure the independence of POT excesses, data larger than x_o should be set so that
164 they are not continuously selected. To ensure this, many studies have performed various
165 clustering processes based on the time interval between extreme events (Gregersen et al.,
166 2017). In this study, individual rainfall events were first separated from the daily rainfall
167 series. The applied Inter-Event Time Definition (IETD) is 1-day (Kim and Han, 2010). Then,
168 in a rainfall event, it was set to select only one value at most as a POT series. For reference, in

https://doi.org/10.5194/hess-2020-167
Preprint. Discussion started: 12 May 2020


Hydrology and Earth System Sciences
Discussions

this study, the threshold x_o for extracting POT excesses was assumed to be constant.

Although studies considering the non-stationarity of the threshold of the POT series have been conducted (Tramblay et al., 2012), in this study, the non-stationarity was given only to the shape parameters of the GP distribution as follows (Um et al., 2017):

$$\alpha_i = e^{\alpha_1 + \alpha_2 Z_i}, \quad (4)$$

where i is the order of occurrence of POT excesses (1 to n), and covariate Z_i is the climate variable corresponding to POT excesses (DPT on the day of POT excesses in this study). Therefore, the parameters of the stationary GP distribution to be estimated are α and k, and the parameters of the non-stationary GP distribution are α_1, α_2, and k.

2.2 Metropolis-Hastings algorithm

The parameters of the GP distribution were estimated using the Metropolis-Hastings (MH) algorithm to account for uncertainty. This algorithm is one of the algorithms for the Markov Chain Monte Carlo (MCMC) sampling, which takes a sample from the posterior distribution of the parameter θ given the observation data Y. The MH algorithm starts with the initial parameter value θ_o. Then, N + M sequences of the parameter θ_i $(i = 1, \cdots, N + M)$ are generated through the following procedure:

1) The candidate parameter θ^* is generated from the proposal distribution $q(\theta^*|\theta_{i-1})$. At this time, the proposal distribution was applied to the truncated normal distribution with mean θ_{i-1} and variance Σ in this study. The upper and lower limits of the truncated normal distirubtion corresponding to the upper and lower limits of the parameters were determined in advance.

2) Calculation of the reference value T for adoption as follows:

$$T = \frac{\pi(Y|\theta^*)q(\theta_{i-1}|\theta^*)}{\pi(Y|\theta_{i-1})q(\theta^*|\theta_{i-1})}, \quad (5)$$

where $\pi(Y|\theta^*)$ and $\pi(Y|\theta_{i-1})$ are the likelihood values in the parameters θ^* and θ_{i-1}, respectively, and are defined as follows:

$$\pi(Y|\theta) \sim \prod_{i=1}^{n} f(x_i), \quad (6)$$

https://doi.org/10.5194/hess-2020-167
Preprint. Discussion started: 12 May 2020


Hydrology and Earth System Sciences
Discussions

where f() is the probability density function of the GP distribution.

3) If $\min(1,T) > u$ is satisfied for a uniform random number u between 0 and 1, $\theta_i = \theta^*$, otherwise $\theta_i = \theta_{i-1}$.

The Markov chain, constructed through the initial N iterations, converges to a chain that randomly samples parameters from the posterior distribution of parameters. At this time, the parameter sampled before the initial N iterations should be discarded.

Before using the MH algorithm, it is necessary to determine the initial parameter θ_o, the proposal distribution $q(\theta^*|\theta_{i-1})$, the initial iterative sampling number N, and the total iterative sampling number N + M. The choice of the initial parameter value θ_o is generally not sensitive to the results, while the choice of the proposal distribution $q(\theta^*|\theta_{i-1})$ is important. The general method is to use a normal distribution with mean θ_{i-1} and a constant covariance matrix Σ. It is recommended to select Σ so that the adoption rate of $\min(1,T) > u$ is 20 to 70 %. The number of iterations to be discarded, N, is known to be sufficient if more than 10 % of M is applied, and the number of samples, M, should be secured enough to track the progress of the chain and converge the average values of the parameter posterior distribution.

The characteristics of the posterior distribution of parameters from the generated samples can be quantified. In general, the final estimated parameter $\bar{\theta}$ is calculated as follows:

$$\bar{\theta} = \frac{1}{M}\sum_{i=N+1}^{N+M}\theta_i. \quad (7)$$

In addition, the variance of the estimated parameters can be calculated from the generated samples.

3. Results

3.1 Selection of POT threshold

Since frequency analysis using POT excesses requires independent rainfall data greater than the threshold x_o, it is necessary to set x_o. One of the most commonly used methods of setting the appropriate x_o is the mean residual life plot (Coles, 2001), and the results of

https://doi.org/10.5194/hess-2020-167
Preprint. Discussion started: 12 May 2020


Hydrology and Earth System Sciences
Discussions

223 applying it to the daily precipitation data at Busan and Seoul sites are shown in Figure 2. In
224 general, a nonlinear curve appears in a section where a small x_o is selected, and an
225 approximate straight line appears as x_o increases. It is recommended to set x_o in this straight
226 section. From Figure 2, it can be found that the appropriate range of x_o is in the range of 30
227 to 150 mm / day for both Busan and Seoul sites. In this study, x_o = 50 mm / day was set as a
228 threshold for the POT series in both Busan and Seoul sites.

229

230 [Figure 2. Mean residual life plot at (a) Busan and (b) Seoul sites.]

231

232 **3.2 Stationary frequency analysis**

233 The parameters of the GP distribution were estimated using the method of probability
234 weighted moments (PWM) and MH algorithm, respectively. Figure 3 shows the result of PWM
235 parameter estimation and the posterior distribution of parameters by the MH algorithm. Since
236 the MH algorithm does not return a single-valued parameter, but estimates the posterior
237 distribution of the parameter, information about the uncertainty of the estimated parameter can
238 be obtained. It can be recognized that the posterior distribution of the scale parameter
239 converged to an appropriate range even though a relatively wide range of uniform distribution
240 was assumed as the prior-distribution (the whole section of the horizontal axis in Figure
241 3). However, in the case of the shape parameter, it can be found that the uncertainty is formed
242 relatively higher. That is, it can be seen that the uncertainty included when fitting the POT
243 series of Busan and Seoul sites to the GP distribution is mainly due to the estimation of the
244 shape parameter.

245

246 [Figure 3. Posterior distribution of parameters of stationary and non-stationary GP distribution.]

247

248 Table 1 shows the final estimated parameters. The parameter estimation value of the MH
249 algorithm was defined as the ensemble average of samples extracted by MCMC from the
250 posterior distribution as mentioned in Eq. (7). The parentheses of the parameter estimation

https://doi.org/10.5194/hess-2020-167
Preprint. Discussion started: 12 May 2020


Hydrology and Earth System Sciences
Discussions

values by the MH algorithm in Table 1 are the coefficient of variation of the parameter. It can be found that the PWM and MH algorithms give similar parameter values for both scale and shape parameters. The negative logarithm likelihood (nllh) was also calculated similarly. From the above results, it can be recognized that when the POT series is to be fit to the GP distribution, parameter estimation by the MH algorithm is applicable, and information about the uncertainty of the estimated parameters is also obtainable.

[Table 1. Parameter estimation of stationary GP distribution]

3.3 Non-stationary frequency analysis

For analyzing the non-stationary frequency of POT excesses, the non-stationary GP distribution, in which the scale parameter was defined as a function of DPT on the day when the POT excesses occurred, was set as in Eq. (4). The parameters of the non-stationary GP distribution were estimated using the MH algorithm, and Figure 3 shows the posterior distribution of the parameters by the MH algorithm. Similar to the stationary GP distribution, the posterior distribution of the scale parameter converged to an appropriate range, although a relatively wide range of prior-distributions was assumed. However, it can be recognized that the uncertainty is still high in the case of the shape parameter.

The scale parameter finally estimated at Busan site using Eq. (7) is $\alpha = \exp[2.2149 + 0.071078 \cdot Z]$ (where Z is DPT), and the shape parameter is k = -0.1123. The coefficient of variation of the scale parameter was 7.66 % when the DPT was given at 20.2576 ℃, and the coefficient of variation of the shape parameter was 44.02 %. Therefore, when compared with the coefficient of variation of the parameters of the stationary GP distribution in Table 1, it can be recognized that the uncertainty in both the scale parameter and the shape parameter slightly decreased in the non-stationary GP distribution. However, in the scale parameter, these coefficients of variation are obtained under the assumption of a specific DPT, so if the range of the observed DPT is reflected, the coefficient of variation of the scale parameter of the non-stationary GP distribution will have a larger value. The AIC of the stationary model was AIC = 3264.84, and the AIC of the non-stationary model was calculated as AIC = 3247.61. From

https://doi.org/10.5194/hess-2020-167
Preprint. Discussion started: 12 May 2020


Hydrology and Earth System Sciences
Discussions

the viewpoint that the AIC of the non-stationary model is slightly smaller, it can be said that the non-stationary model has better performance in expressing the frequency of the POT excesses than the stationary model. The parameter estimation results of Seoul site also showed a similar trend to those of Busan site. In other words, under certain DPT conditions, the uncertainty of the scale and shape parameters of the non-stationary model was slightly reduced than that of the stationary model, and the AIC of the non-stationary model was calculated to be smaller than the AIC of the stationary model.

3.4 Uncertainty analysis

The final goal of frequency analysis is estimation of rainfall quantile, but the parameters of probability distribution required for estimation of quantile as well as quantile are inevitably uncertain since they are estimated from limited samples. Therefore, looking at the parameters of the probability distribution applied and the uncertainty of the quantile derived as a result of frequency analysis gives important information to determine whether the model is applicable. In this study, the following quantitation factors were defined to quantify the uncertainty between the stationary and non-stationary models:

$$\mathrm{m}-\mathrm{factor}=\frac{Width\ of\ 95\ PPU\ for\ parameter}{estimated\ parameter\ value},\ \text{and} \tag{8}$$

$$\mathrm{h}-\mathrm{factor}=\frac{Width\ of\ 95\ PPU\ for\ rianfall\ quantile\ ensemble}{rainfall\ quantile\ estimate}, \tag{9}$$

where 95 PPU means 95 % predicted uncertainty of the corresponding variable (Abbaspour et al., 2007).

A total of 6,000 parameter values were sampled from the posterior distribution of parameters for each of the stationary and non-stationary models, and 6,000 rainfall quantile ensemble corresponding to a return level of 100-year were generated. Eqs. (8) and (9) were used to quantify the uncertainty for parameters and the uncertainty for rainfall quantile. Table 2 shows the results. The parameters of the stationary GP distribution are α and k, whereas the parameters of the non-stationary GP distribution are α_1, α_2, and k, so for direct comparison, m-factor derived by converting α_1 and α_2 of the non-stationary GP distribution to $\alpha=\exp[\alpha_1+\alpha_2 DPT_r]$ were expressed together. Here, DPT_r is a reference DPT, and

https://doi.org/10.5194/hess-2020-167
Preprint. Discussion started: 12 May 2020


Hydrology and Earth System Sciences
Discussions

308 20.2576 ℃ for Busan site and 21.4962 ℃ for Seoul site, respectively. The reference DPT will
309 be discussed in detail in the discussion section.

310

311 [Table 2. Uncertainty of stationary and non-stationary frequency analysis]

312

313 The uncertainty of the parameters was first investigated for the m-factor of Eq. (8). It can
314 be found that the uncertainty of the scale parameter of the non-stationary model is less than the
315 uncertainty of the scale parameter of the stationary model under the condition given the
316 reference DPT (10.9 % at Busan site, and 1.7 % at Seoul site). In the case of the shape parameter,
317 Busan and Seoul sites showed different results. The uncertainty of the non-stationary model
318 decreased at Busan site (10.2%), but increased at Seoul site (9.9%). This suggests that even if
319 a non-stationary model is introduced, it is difficult to expect that the uncertainty resulting from
320 parameter estimation of the GP distribution would be reduced. The fact that the uncertainty in
321 the scale parameter has been shown to be reduced is the result from the condition under which
322 a specific DPT is given, so it would be also difficult to argue that the uncertainty in the scale
323 parameter has been reduced if changes in DPT are reflected.

324 The h-factor of rainfall quantile corresponding to the return level of 100-year was
325 calculated in two ways. First, under the condition given the reference DPT, the h-factor of the
326 non-stationary model was reduced by 37 % (at Busan site) and 28 % (at Seoul site) than the
327 stationary model. However, under the condition that DPT is not given in advance, it can be
328 found that the h-factor of the non-stationary model is calculated to be larger than the h-factor
329 of the stationary model because of the overlapping effects of uncertainty from parameter
330 estimation and DPT change.

331 The results tells us the fact that although the non-stationary model is better in the fitting
332 performance of the data, it is difficult to say that the non-stationary model is more reliable than
333 the stationary model because of the non-stationarity from the variation of the covariate when
334 estimating rainfall quantile. Ouarda et al (2020) also produced similar results using the annual
335 maximum rainfall series and the non-stationary GEV distribution.

336 We are here to note the condition under which DPT is given. In upper left figures in Figure

https://doi.org/10.5194/hess-2020-167
Preprint. Discussion started: 12 May 2020


Hydrology and Earth System Sciences
Discussions

4(a) and (b), it should be noted that while the ensemble average of the stationary rainfall quantile has a single value for a given parameter sample, the non-stationary ensemble average has various values in response to the DPT value on the day of the POT excess. That is, since the change in DPT is additionally reflected in addition to the parameter uncertainty, the range of the ensemble of the non-stationary rainfall quantile is likely to be formed wider than the range of the ensemble of the stationary rainfall quantile. In the upper right figures of Figure 4, it can be found that, while the stationary 95 PPU has a certain range regardless of the state of DPT, the non-stationary 95 PPU is formed over a very wide range depending on the state of DPT. It should be noted, however, that under the given DPT, the range of the non-stationary 95PPU is less than that of the stationary 95 PPU. In the non-stationary frequency analysis, as DPT increases, rainfall quantile estimates increase. That is, if a DPT is given, the quantile ensemble sampled by the MCMC also reflects the state of the given DPT, so not only the ensemble average, but also the lower 2.5 % and upper 97.5 % of the ensemble reflect the state of the given DPT. Since the DPT corresponding to each of the POT excesses constituting the POT series is a known value, the h-factor of the rainfall quantile corresponding to each POT excess can be obtained (see the lower left figures in Figure 4(a) and (b)). If DPT is given, it can be recognized that the non-stationary h-factor is smaller than the stationary h-factor. In other words, under the condition that DPT is given, there is a room to say that the non-stationary frequency analysis is superior to the stationary frequency analysis in terms of reliability. As can be seen in the lower right figures in Figure 4(a) and (b), the frequency distribution of DPT is slightly distorted to the left. Interestingly, it can be found that the mode of DPT frequency distribution is located near DPT where the stationary rainfall quantile ensemble average and the non-stationary rainfall quantile ensemble average are the same at both Busan and Seoul sites.

[Figure 4. Changes in uncertainty for co-variate at (a) Busan and (b) Seoul sites.]

https://doi.org/10.5194/hess-2020-167
Preprint. Discussion started: 12 May 2020


Hydrology and Earth System Sciences
Discussions

364 **4. Discussion**

365 **4.1 Reference dew-point temperature**

366 The formula for rainfall quantile X_T corresponding to the return level of T-year in the
367 non-stationary GP distribution using covariate is as follows:

368 $$X_T = x_o + \frac{1}{k} e^{\alpha_1 + \alpha_2 Z} \left[1 - \left(\frac{1}{\lambda T}\right)^k\right]. \quad (10)$$

369 In other words, rainfall quantile X_T appears as a function of covariate.

370 Figure 5 shows the empirical distribution of rainfall quantile corresponding to the return
371 level of 100-year using DPT observed at Busan and Seoul sites. Note that the non-stationary
372 GP distribution using the covariate returns rainfall quantile of various values depending on the
373 DPT corresponding to the POT excess. As can be seen in Figure 5, the non-stationary frequency
374 analysis can provide an empirical distribution of rainfall quantile in the present condition of
375 DPT and in the future condition of elevated DPT due to global warming. Therefore, the change
376 in rainfall quantile considering global warming can be expressed explicitly. While rainfall
377 extremes derived from climate models have significant bias and uncertainty, DPT can yield
378 relatively reliable climate model outputs (O'Gorman, 2012; Lenderink and Attema, 2015;
379 Farnham et al., 2018). Therefore, it can be said that the non-stationary frequency analysis using
380 DPT has an advantageous structure for examining the effect of global warming on rainfall
381 quantile (Wasko and Sharma, 2017; Lee et al., 2019).

382

383 [Figure 5. Rainfall quantile estimates at (a) Busan and (b) Seoul sites for return level of 100-
384 year using observed dew-point temperature and global warming scenarios.]

385

386 One of the problems to be solved in the non-stationary frequency analysis using a covariate
387 is how to set the value of a reference covariate corresponding to a specific quantile. In practice,
388 it is often required to have a single design rainfall depth, so it is very cumbersome to give the
389 result of calculating the rainfall quantile of various values depending on the change of the
390 DPT. In addition, as described above, when performing an uncertainty analysis of a non-

https://doi.org/10.5194/hess-2020-167
Preprint. Discussion started: 12 May 2020


Hydrology and Earth System Sciences
Discussions

391 stationary frequency analysis, an undesired disturbance in which an ensemble of rainfall
392 quantile is excessively dispersed due to a change in DPT appears. Since the state of DPT is the
393 data observed on the day of POT excess (i.e., deterministic variable), analyzing the uncertainty
394 of rainfall quantile by randomly pulling a DPT from the DPT probability distribution will likely
395 result in overestimating the uncertainty.

396 Figure 6 shows an example of selecting the reference DPT. From Eq. (10), the DPT value
397 (i.e., reference DPT) of the non-stationary GP distribution that returns the rainfall quantile
398 equal to the stationary GP distribution can be calculated. The results of calculating the reference
399 DPT using the POT series at Busan and Seoul sites revealed that the reference DPT increased
400 as the return level increased. From the results of regression analysis of empirical cumulative
401 probability of observed DPTs and return level, a relationship of F(DPT) = 0.4900RL^0.05189
402 was obtained at Busan site, and F(DPT) = 0.4027RL^0.1021 at Seoul site (where RL is the
403 return level in year). The coefficient of determination of the regression analysis was 0.97 at
404 Busan site and 0.99 at Seoul site. From these results, the reference DPT corresponding to the
405 return level of 100-year at Busan site could be applied to 20.2576 ℃ and Seoul site to
406 21.4962 ℃. The choice of reference covariate may be an important research topic in the
407 frequency analysis of covariate-based anomalies.

408

409 [Figure 6. Selection of reference dew-point temperature for estimating rainfall quantiles at (a)
410 Busan and (b) Seoul sites.]

411

412 The uncertainty of the non-stationary frequency analysis for various sample size changes
413 was analyzed using a reference DPT corresponding to the return level of 100-year. In the first
414 case, POT and covariate series of the last 10 years from 2008 to 2017 were applied, and
415 frequency analysis was performed by extending the data period in the past direction for 5
416 years. Figure 7 shows the uncertainty of rainfall quantile under the condition that the reference
417 DPT is given. Generally, the h-factor of the non-stationary frequency analysis is smaller than
418 the stationary frequency analysis. It can be found that for the h-factor to be less than 0.5, the
419 non-stationary frequency analysis requires a data period of about 40 years (at Busan site) and

https://doi.org/10.5194/hess-2020-167
Preprint. Discussion started: 12 May 2020


Hydrology and Earth System Sciences
Discussions

420 75 years (at Seoul site), while the stationary frequency analysis requires more than 100 years.
421 These results indicate that the reliability of the non-stationary frequency analysis may be
422 superior to the reliability of the stationary frequency analysis under the condition that an
423 appropriate reference DPT is given.

424

425 [Figure 7. Effect of the number of samples on the uncertainty of rainfall quantile using
426 reference dew-point temperature.]

427

428 **4.2 Uncertainty of rate of change**

429 Through Figure 5, we have seen that the non-stationary frequency analysis using DPT has
430 an advantageous structure for examining the effect of global warming on rainfall quantile. In
431 this section, we extend the concept of Figure 5 a little further to investigate the uncertainty
432 about the rate of change in rainfall quantile for global warming. Here, the rate of change is
433 defined as [future rainfall quantile - present rainfall quantile] / [present rainfall quantile]. That
434 is, a rate of change of 0.2 means that the future rainfall quantile will increase by 20 % from the
435 present rainfall quantile. In most global warming scenarios, the state of DPT increases, so the
436 case where the change rate is less than 0 is not considered in this study. In fact, it is not difficult
437 to consider.

438 Let us assume that rainfall quantile for the return level of T-year in the present DPT state
439 is X_p^T, and rainfall quantile in the future DPT state is X_f^T. At this time, X_p^T and X_f^T are
440 composed of ensemble sampled by MCMC under the conditions given the present and future
441 reference DPT, respectively. The probability that the rainfall quantile X_f^T in the future DPT
442 state increases more than $\alpha\times100$ (%) than the rainfall quantile X_p^T in the present DPT
443 condition, that is, the probability P_α^T that the rate of change becomes more than α can be
444 defined as follows:

445 $$P_\alpha^T = P\left[X_f^T \geq (1+\alpha)X_p^T\right] = 1 - \int_0^\infty F_f^T\left[(1+\alpha)X_p^T\right] \cdot f_p^T\left[X_p^T\right] dX_p^T, \qquad (11)$$

446 where $F_f^T[]$ is the cumulative probability distribution function of X_f^T in the future DPT state,
447 and will behave depending on the DPT rise in the future global warming scenario. The

https://doi.org/10.5194/hess-2020-167
Preprint. Discussion started: 12 May 2020


Hydrology and Earth System Sciences
Discussions

probability distribution of X_p^T in the present DPT state was expressed as $f_p^T[]$. From Eq. (11), it can be recognized that P_α^T increases as the future DPT increase increases, and decreases as the rate of change increases.

When frequency analysis using the Bayesian approach is performed, a large number of samples for X_p^T and X_f^T can be obtained through MCMC simulation, so instead of calculating P_α^T using Eq. (11), it is possible to numerically calculate P_α^T from the generated samples. Figure 8 shows the probability that the rainfall quantile for the return level of 100-year will exceed a certain rate of change under various conditions (ΔDPT) in a global warming scenario expressed as a rise in DPT. That is, the probability that the rainfall quantile for the return level of 100-year increases by 20 % or more in a scenario condition in which the state of DPT increases by 6 ℃ at Busan site is about 80 %.

[Figure 8. Likelihood of increase over change rate of rainfall quantile for return level of 100-year.]

When Figure 8 is substituted for a specific DPT rise scenario, the reliability of the rate of change in rainfall quantile can be obtained as explained below. Figure 9 describes the procedure for analyzing the rate of change in rainfall quantile for the return level of 100-year under the DPT 4 ℃ rise scenario. The upper left figures in Figure 9(a) and (b) show the probability distribution of rainfall quantile ensemble at Busan and Seoul sites, respectively. One can see that the probability distribution of X_f^T is shifted to the right. Using the concept of Eq. (11), likelihood of increase over change rate (LoI), P_α^T, can be drawn from the information on these probability distributions as shown in the upper right. Since LoI is the probability that the rate of change of rainfall quantile for a specific return level is greater than or equal to α in a specific DPT rising condition, the probability that the rate of change will be less than or equal to α is $1 - P_\alpha^T$. That is, the cumulative probability distribution of rate of change becomes $1 - P_\alpha^T$, which is shown in the lower right. The probability distribution of rate of change can be obtained numerically from the cumulative probability distribution of rate of change, and it is shown in the lower left. The ensemble average of the rate of change of rainfall quantile for

https://doi.org/10.5194/hess-2020-167
Preprint. Discussion started: 12 May 2020


Hydrology and Earth System Sciences
Discussions

the return level of 100-year at Busan site was 0.3138 (0.3742 at Seoul site) and the standard deviation of the ensemble was 0.2734 (0.3298 at Seoul site).

[Figure 9. Procedure for analyzing uncertainty in rate of change.]

The uncertainty of the parameters estimated in the frequency analysis will influence the estimation of the rate of change in future climate change scenarios. An ensemble of rainfall quantile can be obtained from various parameter combinations sampled by MCMC, and an ensemble of future rainfall quantile can also be obtained by applying climate change scenarios to covariates. A simple comparison of the ensemble average of rainfall quantile derived from present and future DPT states using a reference DPT makes it possible to obtain an average rate of change, but it is impossible to determine how reliable the rate of change is. Through the procedure presented in Figure 9, one can recognize that it is possible to quantify the uncertainty inherent in the rate of change. It should be noted, however, that this uncertainty analysis of rate of change only considered the uncertainty that comes from parameter estimation. When analyzing the uncertainty of the rate of change, the uncertainty arising from the selection of probability distributions for frequency analysis and the uncertainty resulting from the choice of covariates should also be addressed. In addition, the uncertainty arising from various climate change scenarios should be treated as important.

5. Conclusion

Natural environmental changes, such as global warming, have a serious impact on the assumptions of the stationarity of the observations. Non-stationarity is an important issue that can never be ignored in areas related to drainage system design, as it can alter the design flood volume obtained using the stationary frequency analysis of observed rainfall extremes. In this study, the stationary and non-stationary frequency analysis was performed using daily precipitation data at Busan and Seoul sites in Korea.

Daily precipitation data for frequency analysis was extracted based on the POT

https://doi.org/10.5194/hess-2020-167
Preprint. Discussion started: 12 May 2020


Hydrology and Earth System Sciences
Discussions

505 approach. As a threshold for extracting the POT series, it was confirmed that a value between
506 30 and 150 mm / day was appropriate from the results of plotting the Mean residual life
507 plot. Both Busan and Seoul site have finally set 50 mm / day as the threshold of the POT
508 excesses. The POT series was adapted to the GP distribution, and as a result of estimating the
509 parameters using the PWM and MH algorithms, it was confirmed that the parameter estimation
510 of the GP distribution by the MH algorithm is applicable. Confirmation of applicability to the
511 MH algorithm means that information on the empirical probability distribution of the estimated
512 GP distribution parameters can be obtained.

513 The non-stationarity of the POT series was implemented by expressing the scale parameter
514 of the GP distribution as a function of the DPT observed on the day of the POT excess. The
515 AIC of the non-stationary GP distribution using the covariate was calculated to be slightly
516 smaller than the AIC of the stationary GP distribution. However, since the difference was
517 thought to be likely to change in any way during the parameter estimation process, it was
518 recognized that the performance in terms of data fitness of the stationary and non-stationary
519 GP distributions was almost similar. Meanwhile, since the non-stationary frequency analysis
520 using DPT can present the empirical distribution of rainfall quantile in the present DPT state
521 and in the DPT rising state due to global warming, it was found that changes in rainfall quantile
522 considering climate change could be explicitly presented.

523 In this study, rainfall quantile for various parameter combinations was simulated using
524 MCMC sampling from the posterior distribution of parameters derived by the MH
525 algorithm. Under the condition considering all observed ranges of DPT, it was found that the
526 uncertainty of the non-stationary model was calculated to be greater than the uncertainty of the
527 stationary model since the variability caused by DPT was added to the uncertainty resulting
528 from parameter estimation. In other words, although the performance in terms of goodness of
529 fit was better for the non-stationary model, it was difficult to say that the results of the non-
530 stationary model were more reliable than the results of the stationary model because of the non-
531 stationarity from the variation of the covariate when estimating rainfall quantile. However, in
532 this study, the concept of reference DPT was introduced to prevent excessive dispersion of
533 rainfall quantile ensemble due to changes in DPT. That is, it was suggested that the reliability
534 of the non-stationary frequency analysis might be superior to the reliability of the stationary
535 frequency analysis under the condition that an appropriate reference DPT is given. For

https://doi.org/10.5194/hess-2020-167
Preprint. Discussion started: 12 May 2020


Hydrology and Earth System Sciences
Discussions

reference, it was found that it was necessary to increase the reference DPT in response to the return level of the rainfall quantile.

The main focus of this study was on how to examine the relative superiority of the stationary and non-stationary models when performing frequency analysis. When considering the uncertainty of the parameter of probability distribution, which is mainly caused by the limited sample size, it was thought be insufficient to evaluate the relative goodness of the stationary and non-stationary models only by evaluating the fitness of the sample using the estimated parameter. This study was promoted from the viewpoint that a model with smaller uncertainty inherent in rainfall quantile, which is the result of frequency analysis, was better. From this point of view, it was found that the DPT-based non-stationary frequency analysis could be a better model than the stationary frequency analysis if the reference DPT was properly given. In addition, it was recognized that the uncertainty of the rate of change of rainfall quantile in future DPT conditions could also be identified by using the rainfall quantile ensemble in present and future DPT conditions that can be obtained in the uncertainty analysis process.

https://doi.org/10.5194/hess-2020-167
Preprint. Discussion started: 12 May 2020

Hydrology and Earth System Sciences
Discussions
Open Access
EGU

Acknowledgments

This work was supported by the National Research Foundation of Korea (NRF) grant funded by the Korea government (MSIT) (No. NRF-2019R1A2C1003114).

References

Abbaspour, K., Yang, J. Maximov, I., Siber, R., Bogner, K, Mieleitner, J. and Srinivasan, R. (2007) Modelling hydrology and water quality in the pre-Alpine/Alpine thur watershed using SWAT, Journal of Hydrology, 333, pp. 413-430.

Agilan V. and Umamahesh, N. (2016) Modelling nonlinear trend for developing non-stationary rainfall intensity-duration-frequency curve. International Journal of Climatology, 37, pp. 1265-1281.

Agilan, V. and Umamahesh, N. (2017) What are the best covariates for developing nonstationary rainfall Intensity-Duration-Frequency relationship? Advances in Water Resources, 101, pp. 11-22.

Agilan V. and Umamahesh, N. (2018) Covariate and parameter uncertainty in non-stationary rainfall IDF curve, International Journal of Climatology, 38, pp. 365-383.

Akaike, H. (1974) A new look at the statistical model identification. IEEE transactions on automatic control, 19, pp. 716-723.

Alexander, L., Zhang, X., Peterson, T., Gleason, J., Tank, A., Haylock, M., Collins, D., Trewin, B., Rahimzadeh, F., Tagipour, A., Kumar, K., Revadekar, J., Griffiths, G., Vincent, L., Stephenson, D., Burn, J., Aguilar, E., Brunet, M., Taylor, M., Zhai, M., Rusticucci, M. and Vazquez-Aguirre, J. (2006) Global observed changes in daily climate extremes of temperature and precipitation. Journal of Geophysical Research - Atmospheres, 111, pp. 1-22.

Berg, P., Moseley, C. and Haerter, J. (2013) Strong increase in convective precipitation in response to higher temperatures. Nature Geoscience, 6, pp. 181-185.

Cheng, L., AghaKouchak, A., Gilleland, E. and Katz, R. (2014) Non-stationary extreme value analysis in a changing climate. Climate Change, 127(2), pp. 353-369.

Choi, H., Kwon, H. and Park, M. (2019) A development of nonstationary rainfall frequency analysis model based on mixture distribution. Journal of Korea Water Resources Association, 52(11), pp. 895-904. [Korean Literature]

Choi, J, Lee, J. and Kim, S. (2019) Impact of Sea Surface Temperature and Surface Air Temperature on Maximizing Typhoon Rainfall: Focusing on Typhoon Maemi in Korea. 2019, Article ID 1930453, https://doi.org/10.1155/2019/1930453.

Choi, J., Lee, O., Jang, J., Jang, S. and Kim, S. (2019) Future intensity-depth-frequency curves estimation in Korea under representative concentration pathway scenarios of Fifth

https://doi.org/10.5194/hess-2020-167
Preprint. Discussion started: 12 May 2020

assessment report using scale-invariance method. International Journal of Climatology, 39(2), pp. 887-900.

Coles, S. (2001) An introduction to statistical modeling of extreme value. Heidelberg: Springer-Verlag.

Coles, S., Bawa, J., Trenner, L. and Dorazio, P. (2001) An Introduction to Statistical Modeling of Extreme Values. Springer, London.

Cunha, L., Krajewski, W., Mantilla, R. and Cunha, L. (2011) A framework for flood risk assessment under nonstationary conditions or in the absence of historical data. Journal of Flood Risk Management, 4, pp. 3-22.

Das, T., Dettinger, M., Cayan, D. and Hidalgo, H. (2011) Potential increase in floods in California's Sierra Nevada under future climate projections. Climate Change, 109, pp. 71-94.

DeGaetano, A. (2009) Time-dependent changes in extreme-precipitation return period amounts in the continental United States. Journal of Applied Meteorology, 48, pp. 2086-2098.

Emori, S. and Brown, S. (2005) Dynamic and thermodynamic changes in mean and extreme precipitation under changed climate. Geophysical Research Letters, 32, L17706.

Farnham, D., Doss-Gollin, J. and Lall, U. (2018) Regional extreme precipitation events: Robust inference from credibly simulated GCM variables. Water Resources Research, 54(6), pp. 3809-3824.

Ganguli, P. and Coulibaly, P. (2017) Does nonstationarity in rainfall require nonstationary intensity-duration-frequency curves? Hydrology and Earth System Sciences, 21(12), pp. 6461-6483.

Graler, B, Berg, M., Vandenberghe, S., Petroselli, A., Grimaldi, S., Baets, B. and Verhoest, N. (2013) Multivariate return periods in hydrology: a critical and practical review focusing on synthetic design hydrograph estimation. Hydrology and Earth System Sciences, 17(4), pp. 1281-1296.

Gregersen, I., Madsen, H., Rosbjerg, D. and Arnbjerg-Nielsen, K. (2013) A spatial and nonstationary model for the frequency of extreme rainfall events. Water Resources Research, 49, pp. 127-136.

Gregersen, I., Madsen, H., Rosbjerg, D. and Arnbjerg-Nielsen, K. (2017) A regional and nonstationary model for partial duration series of extreme rainfall. Water Resources Research, 53(4), pp. 2659-2678.

Groisman, P., Knight, R. and Karl, T. (2012) Changes in intense precipitation over the central United States. Journal of Hydrometeorology, 13, pp. 47-66.

Haddad, K., Rahman, A. and Green, J. (2011) Design rainfall estimation in Australia: a case study using L moments and generalized least squares regression. Stochastic Environmental Research and Risk Aanlysis, 25, pp. 815-825.

Hao, Z., AghaKouchak, A. and Phillips, T. (2013) Changes in concurrent monthly precipitation and temperature extremes. Environtal Research Letters, 8, 034014.

https://doi.org/10.5194/hess-2020-167
Preprint. Discussion started: 12 May 2020

628 Hassanzadeh, E., Nazemi, A. and Elshorbagy, A. (2013) Quantile-Based Downscaling of
629 Precipitation Using Genetic Programming: Application to IDF Curves in Saskatoon.
630 Journal of Hydrologic Engineering, 19, pp. 943-955.

631 Hosking, J. and Wallis, J. (1987) Parameter and quantile estimation for the generalized Pareto
632 distribution. Technometrics, 29(3), pp. 339-349.

633 Hosking, J. and Wallis, J. (2005) Regional frequency analysis: an approach based on L-
634 moments. Cambridge University Press.

635 Hosseinzadehtalaei, P., Tabari, H. and Willems, P. (2017) Uncertainty assessment for climate
636 change impact on intense precipitation: how many model runs do we need? International
637 Journal of Climatology, 37, pp. 1105-1117.

638 Iliopoulou, T., Koutsoyiannis, D. and Montanari, A., (2018) Characterizing and modeling
639 seasonality in extreme rainfall. Water Resources Research. 54, pp. 6242-6258.

640 Jang, H., Kim, S. and Heo, J. (2015) Comparison study on the various forms of scale parameter
641 for the nonstationary gumbel model. Journal of Korea Water Resources Association, 45(5),
642 pp. 331-343. [Korean Literature]

643 Jung, B., Lee, O., Kim, K. and Kim, S. (2018) Non-stationary frequency analysis of extreme
644 sea level using POT approach. Journal of Korean Society of Hazard Mitigation, 18(7), pp.
645 631-638. [Korean Literature]

646 Jongman, B., Hochrainer-Stigler, S., Feyen, L., Aerts, J., Mechler, R., Botzen, W., Bouwer, L.,
647 Pflug, G., Rojas, R. and Ward, P. (2014) Increasing stress on disaster risk finance due to
648 large floods. Nature Climate Change, 4, pp. 264-268.

649 Karl, T. and Knight, R. (1998) Secular trends of precipitation amount, frequency, and intensity
650 in the United States. Bulletin of the American Meteorological Society, 79, pp. 231-241.

651 Karl, T., Melillo, J. and Peterson, T. (2009) Global climate change impacts in the United States.
652 Cambridge University Press, New York.

653 Kim, H., Kim, T., Shin, H. and Heo, J. (2017) A study on a tendency of parameters for
654 nonstationary distribution using ensemble empirical mode decomposition method. Journal
655 of Korea Water Resources Association, 50(4), pp. 253-261. [Korean Literature]

656 Kim, K., Choi, J., Lee, O., Cha, D. and Kim, S. (2020) Uncertainty quantification of future
657 design rainfall depths in Korea. Atmosphere, 11, 22; doi:10.3390/atmos11010022.

658 Kim, S. and Han, S. (2010) Urban stormwater capture curve using three-parameter mixed
659 exponential probability density function and NRCS runoff curve number method. Water
660 Environment Research, 82(1), pp. 43-50.

661 Kunkel, K., Karl, T., Easterling, D., Redmond, K., Young, J., Yin, X. and Hennon, P. (2013)
662 Probable maximum precipitation and climate change. Geophysical Research Letters, 40,
663 pp. 1402-1408.

664 Lee, O. and Kim, S. (2018) Estimation of future probable maximum precipitation in Korea
665 using multiple regional climate models. Water, 10, 637; doi:10.3390/w10050637.

https://doi.org/10.5194/hess-2020-167
Preprint. Discussion started: 12 May 2020

Lee, O., Park, Y., Kim, E. and Kim, S. (2016) Projection of Korean Probable Maximum Precipitation under Future Climate Change Scenarios. Advances in Meteorology, 2016, ID 3818236.

Lee, O., Sim, I. and Kim, S. (2018) Non-stationary frequency analysis of dialy rainfall depth using climate variable. Journal of Korean Society of Hazard Mitigation, 18(7), pp. 639-647. [Korean Literature]

Lee, O., Sim, I. and Kim, S. (2019) Application of the non-stationary peak-over-threshold methods for deriving rainfall extremes from temperature projections. Journal of Hydrology, https://doi.org/10.1016/ j.jhydrol.2019.124318.

Lenderink, G. and Attema, J. (2015), A simple scaling approach to produce climate scenarios of local precipitation extremes for the Netherlands. Environmental Research Letters, 10(8), 085001, doi:10.1088/1748-9326/10/8/085001.

Madsen, H., Arnbjerg-Nielsen, K. and Mikkelsen, P. (2009) Update of regional intensity-duration-frequency curves in Denmark: tendency towards increased storm intensities. Atmospheric Research, 92, pp. 343-349.

Madsen, H., Mikkelsen, P., Rosbjerg, D. and Harremoes, P. (2002) Regional estimation of rainfall intensity-duration-frequency curves using generalized least squares regression of partial duration series statistics. Water Resources Research, 38, pp. 1-11.

Min, S., Zhang, X., Zwiers, F. and Hegerl, G. (2011) Human contribution to more intense precipitation extremes. Nature, 470, pp. 378-381.

Moon, J., Moon, Y. and Kwon, H. (2016) Assessment of uncertainty associated with parameter of gumbel probability density function in rainfall frequency analysis, Journal of Korea Water Resources Association, 49(5), pp. 411-422. [Korean Literature]

O'Gorman, P. (2012), Sensitivity of tropical precipitation extremes to climate change. Nature Geoscience, 5(10), 697, doi:10.1038/ngeo1568.

Ouarda, T., Yousef, L. and Charron, C. (2019) Non-stationary intensity-duration-frequency curves integrating information concerning teleconnections and climate change. International Journal of Climatology, 39(4), pp. 2306-2323.

Ouarda, T, Charron C. and St-Hilaire, A. (2020) Uncertainty of stationary and nonstationary models for rainfall frequency analysis. International Journal of Climatology, https://doi.org/10.1002/joc.6339.

Salas, J. and Obeysekera, J. (2013) Revisiting the concepts of return period and risk for nonstationary hydrologic extreme events. Journal of Hydrologic Engineering, 19, pp. 554-568.

Salvadori, G. and DeMichele, C. (2010) Multivariate multiparameter extreme value models and return periods: A copula approach. Water Resources Research, 46, pp. 1-11.

Sen, S., He, J. and Kasiviswanathan, K. (2020) Uncertainty quantification using the particle filter for non-stationary hydrological frequency analysis. Journal of Hydrology, 584, 12466, https://doi.org/10.1016/ j.jhydrol.2020.124666.

https://doi.org/10.5194/hess-2020-167
Preprint. Discussion started: 12 May 2020

Hydrology and Earth System Sciences
Discussions

Serinaldi, F. and Kilsby, C. (2015) Stationarity is undead: uncertainty dominates the distribution of extremes. Advances in Water Resources, 77, pp. 17-36.

Shin, H., Ahn, H. and Heo, J. (2014) A study on the changes of return period considering nonstationary of rainfall data. Journal of Korea Water Resources Association, 47(5), pp. 447-457. [Korean Literature]

Sim, I., Lee, O. and Kim, S. (2019) Sensitivity analysis of extreme daily rainfall depth in summer season on surface air temperature and dew-point temperature. Water, 11, 771; doi:10.3390/w11040771.

Sugahara, S., Da Rocha, R. and Silveira, R. (2009) Non-stationary frequency analysis of extreme daily rainfall in Sao Paulo, Brazil. International Journal of Climatology, 29, pp. 1339-1349.

Tramblay, Y., Neppel, L., Carreau, J. and Najib, K. (2013) Non-stationary frequency analysis of heavy rainfall events in southern France. Hydrological Sciences Journal, 58(2), pp. 280-294.

Tramblay, Y., Neppel, L., Carreau, J. and Sanchez-Gomez, E. (2012) Extreme value modelling of daily areal rainfall over Mediterranean catchments in a changing climate. Hydrological Process, 26(25), pp. 3934-3944.

Trenberth, K. (2011) Changes in precipitation with climate change. Climate Research, 47, pp. 123-138.

Um, M., Kim, Y., Markus, M. and Wuebbles, D. (2017) Modeling nonstationary extreme value distributions with nonlinear functions: an application using multiple precipitation projections for US cities. Journal of Hydrology, 552, pp. 396-406.

Wasko, C. and Sharma, A. (2017), Continuous rainfall generation for a warmer climate using observed temperature sensitivities. Journal of Hydrology, 544, pp. 575-590.

Willems, P. (2013) Adjustment of extreme rainfall statistics accounting for multidecadal climate oscillations. Journal of Hydrology, 490, pp. 126-133.

Yilmaz, A., Hossain, I. and Perera, B. (2014) Effect of climate change and variability on extreme rainfall intensity-frequency-duration relationships: a case study of Melbourne. Hydrology Earth System Sciences, 18(10), pp. 4065-4076

Yilmaz, A. and Perera, B. (2013) Extreme Rainfall Nonstationarity Investigation and Intensity-Frequency-Duration Relationship. Journal of Hydrologic Engineering, 19, pp. 1160-1172.

Zhang, X., Wang, J., Zwiers, F. and Groisman, P. (2010) The influence of large-scale climate variability on winter maximum daily precipitation over North America. Journal of Climate, 23, 2902-2915.

https://doi.org/10.5194/hess-2020-167
Preprint. Discussion started: 12 May 2020

Hydrology and Earth System Sciences
Discussions
Open Access
EGU

740 **Table captions:**

741

742 **Table 1. Parameter estimation of stationary GP distribution**

743 **Table 2. Uncertainty of stationary and non-stationary frequency analysis**

744

https://doi.org/10.5194/hess-2020-167
Preprint. Discussion started: 12 May 2020

Hydrology and Earth System Sciences
Discussions
Open Access
EGU

745 **Table 1. Parameter estimation of stationary GP distribution**

Site	Parameter	PWM	MH
Busan	α	33.5972	33.966 (8.54 %)
	k	-0.1423	-0.1477 (47.44 %)
	nllh	1630.38	1630.42
Seoul	α	34.9666	35.1785 (8.93 %)
	k	-0.1633	-0.1772 (38.59 %)
	nllh	1340.82	1340.87

746

747 **Table 2. Uncertainty of stationary and non-stationary frequency analysis**

Site	factor	Parameter	stationary	non-stationary
Busan	m − factor	α_1	0.3278	0.5463
		α_2		0.8700
		α		0.2920
		k	1.7507	1.5717
	h − factor	100-yr	0.7595	0.4771 (1.0274)
Seoul	m − factor	α_1	0.3407	0.7127
		α_2		0.8588
		α		0.3349
		k	1.4204	1.5613
	h − factor	100-yr	0.7421	0.5331 (1.0273)

748

749

https://doi.org/10.5194/hess-2020-167
Preprint. Discussion started: 12 May 2020

Hydrology and Earth System Sciences
Discussions

Figure captions:

Figure 1. Sensitivity of 95 % daily rainfall depth to dew-point temperature at (a) Busan and (b) Seoul sites.

Figure 2. Mean residual life plot at (a) Busan and (b) Seoul sites.

Figure 3. Posterior distribution of parameters of stationary and non-stationary GP distribution. (a) Scale and (b) shape parameters at Busan site, and (c) scale and (d) shape parameters at Seoul site. The black vertical lines are a parameter calculated by PWM, which is expressed as a single value. The posterior distribution of parameters for the stationary GP distribution sampled using the MH algorithm is indicated by red lines. The posterior distribution of parameters for the non-stationary GP distribution is indicated by blue lines. The scale parameter of the non-stationary GP distribution using covariate is defined as a function of DPT. Therefore, the posterior distribution of the scale parameters were derived on the assumption that DPT was given at 20.2576 ℃ (Busan site) and 21.4962 ℃ (Seoul site), respectively.

Figure 4. Changes in uncertainty for co-variate at (a) Busan and (b) Seoul sites. The upper left figures in Figure 4(a) and (b) show the POT series (blank line), and the ensemble average of stationary (blue line) and non-stationary (red line) rainfall quantile corresponding to the return level of 100-year. In the upper right figures, the ensemble average (blue line for stationary model, and red line for non-stationary model), and 95PPU of the stationary (blue dotted line) and non-stationary (red dotted line) rainfall quantile for the return level of 100-year are shown. The lower left figures show the h-factor of the stationary (blue line) and non-stationary (black line) rainfall quantile corresponding to the return level of 100-year. Red lines mean the average of black line. The lower right figures show the histogram of DPT corresponding to POT excesses.

Figure 5. Rainfall quantile estimates at (a) Busan, and (b) Seoul sites for return level of 100-year using observed dew-point temperature and global warming scenarios. The stationary rainfall quantile is indicated as a blue vertical line since it is a single value. The non-stationary rainfall quantiles were calculated using the average of the parameter ensemble sampled by MCMC and the DPT observed on the day of POT excesses (red dotted line). In this figures, 'NS (3 ℃ up)' is an empirical distribution of rainfall quantile derived using DPTs that add 3 ℃ to DPTs observed on the day of POT excesses. Likewise, 'NS (5 ℃ up)' is an empirical distribution of rainfall quantile under the scenario condition where DPT has risen 5 ℃ due to global warming.

Figure 6. Selection of reference dew-point temperature for estimating rainfall quantiles at (a) Busan and (b) Seoul sites. In this figure, 'F(DPT)' refers to the empirical cumulative probabilities of DPT on the day of POT excess.

Figure 7. Effect of the number of samples on the uncertainty of rainfall quantile using reference dew-point temperature.

Figure 8. Likelihood of increase over change rate of rainfall quantile for return level of 100-year.

https://doi.org/10.5194/hess-2020-167
Preprint. Discussion started: 12 May 2020

Hydrology and Earth System Sciences
Discussions
Open Access
EGU

784 **Figure 9. Procedure for analyzing uncertainty in rate of change. In upper left figures, the blue line is the**
785 **probability distribution of X_p^T in the present condition, and the red line is the probability distribution of**
786 **X_f^T in the DPT 4 ℃ rising condition. In the lower left figures, the section of the standard deviation was**
787 **colored in pink.**

788

789

https://doi.org/10.5194/hess-2020-167
Preprint. Discussion started: 12 May 2020

Hydrology and Earth System Sciences
Discussions

790

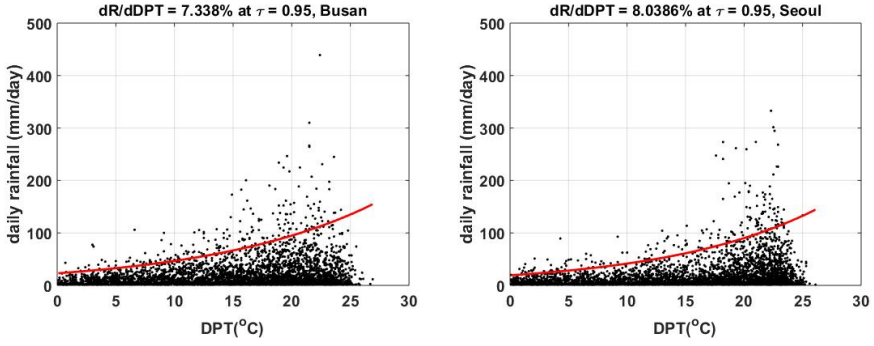

791

792 **(a)** **(b)**

793 **Figure 1. Sensitivity of 95 % daily rainfall depth to dew-point temperature at (a) Busan and (b) Seoul sites.**

794

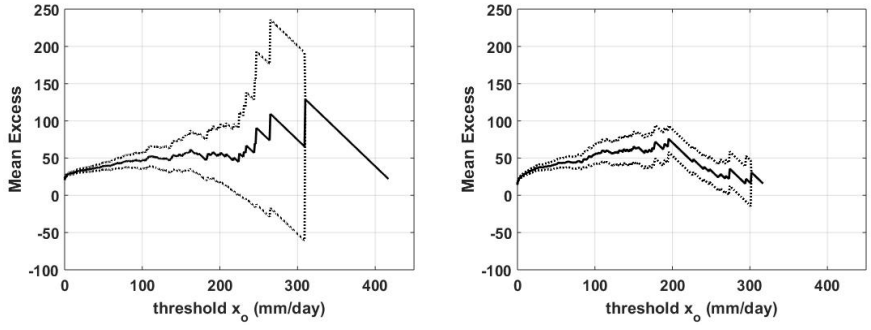

795

796 **(a)** **(b)**

797 **Figure 2. Mean residual life plot at (a) Busan and (b) Seoul sites.**

798

799

https://doi.org/10.5194/hess-2020-167
Preprint. Discussion started: 12 May 2020

Hydrology and Earth System Sciences
Discussions

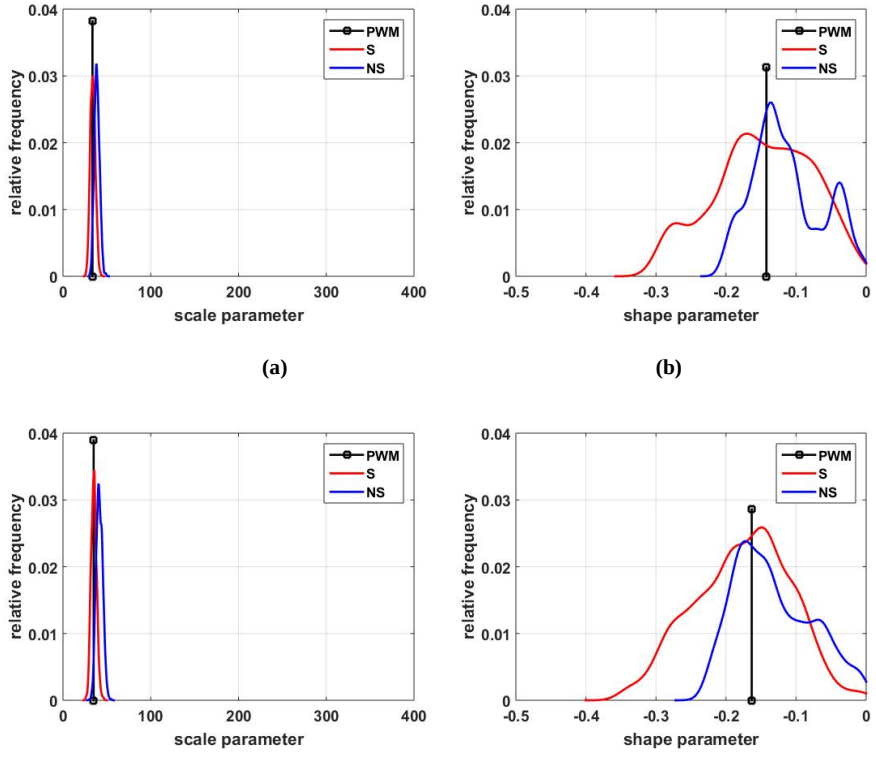

Figure 3. Posterior distribution of parameters of stationary and non-stationary GP distribution. (a) Scale and (b) shape parameters at Busan site, and (c) scale and (d) shape parameters at Seoul site. The black vertical lines are a parameter calculated by PWM, which is expressed as a single value. The posterior distribution of parameters for the stationary GP distribution sampled using the MH algorithm is indicated by red lines. The posterior distribution of parameters for the non-stationary GP distribution is indicated by blue lines. The scale parameter of the non-stationary GP distribution using covariate is defined as a function of DPT. Therefore, the posterior distribution of the scale parameters were derived on the assumption that DPT was given at 20.2576 ℃ (Busan site) and 21.4962 ℃ (Seoul site), respectively.

https://doi.org/10.5194/hess-2020-167
Preprint. Discussion started: 12 May 2020

Hydrology and Earth System Sciences
Discussions

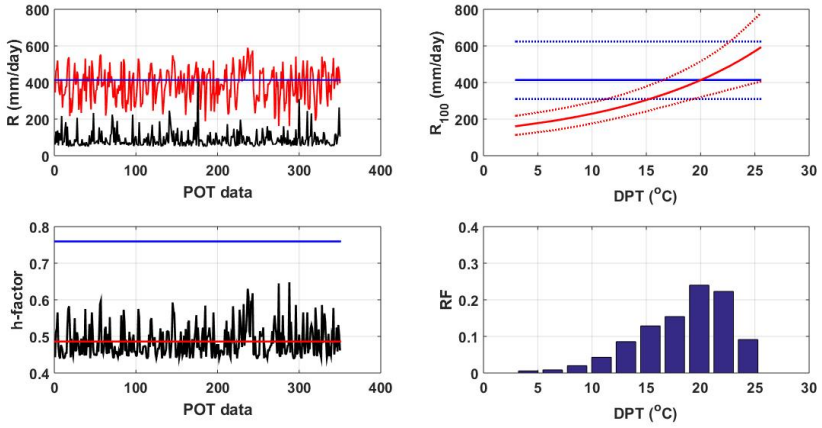

(a)

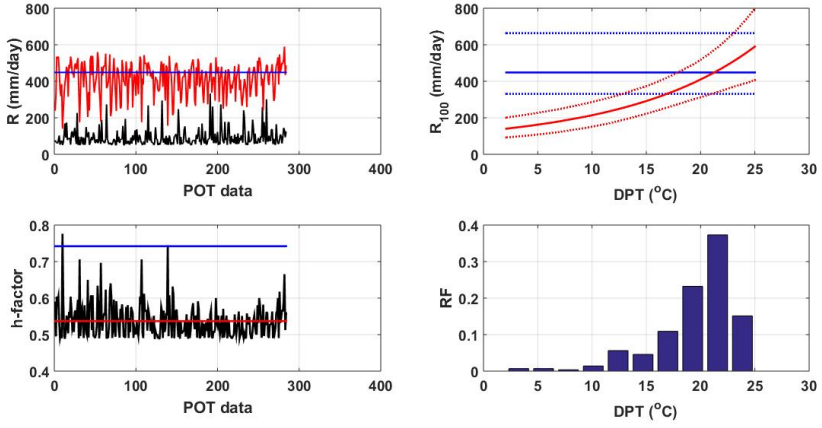

(b)

Figure 4. Changes in uncertainty for co-variate at (a) Busan and (b) Seoul sites. The upper left figures in Figure 4(a) and (b) show the POT series (blank line), and the ensemble average of stationary (blue line) and non-stationary (red line) rainfall quantile corresponding to the return level of 100-year. In the upper right figures, the ensemble average (blue line for stationary model, and red line for non-stationary model), and 95PPU of the stationary (blue dotted line) and non-stationary (red dotted line) rainfall quantile for the return level of 100-year are shown. The lower left figures show the h-factor of the stationary (blue line) and non-stationary (black line) rainfall quantile corresponding to the return level of 100-year. Red lines mean the average of black line. The lower right figures show the histogram of DPT corresponding to POT excesses.

https://doi.org/10.5194/hess-2020-167
Preprint. Discussion started: 12 May 2020

Hydrology and Earth System Sciences
Discussions

826

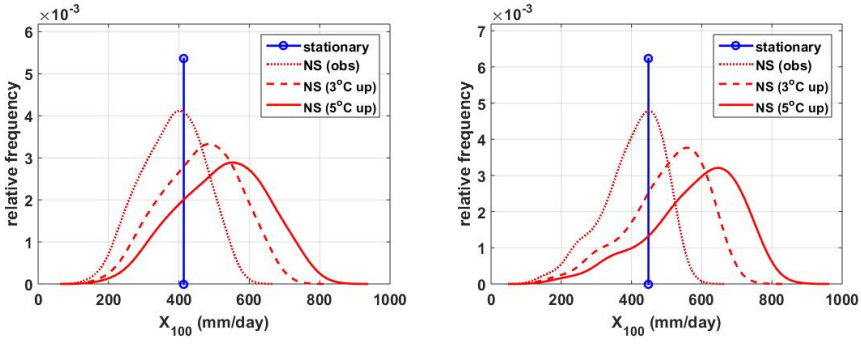

827

828

Figure 5. Rainfall quantile estimates at (a) Busan, and (b) Seoul sites for return level of 100-year using observed dew-point temperature and global warming scenarios. The stationary rainfall quantile is indicated as a blue vertical line since it is a single value. The non-stationary rainfall quantiles were calculated using the average of the parameter ensemble sampled by MCMC and the DPT observed on the day of POT excesses (red dotted line). In this figures, 'NS (3 ℃ up)' is an empirical distribution of rainfall quantile derived using DPTs that add 3 ℃ to DPTs observed on the day of POT excesses. Likewise, 'NS (5 ℃ up)' is an empirical distribution of rainfall quantile under the scenario condition where DPT has risen 5 ℃ due to global warming.

837

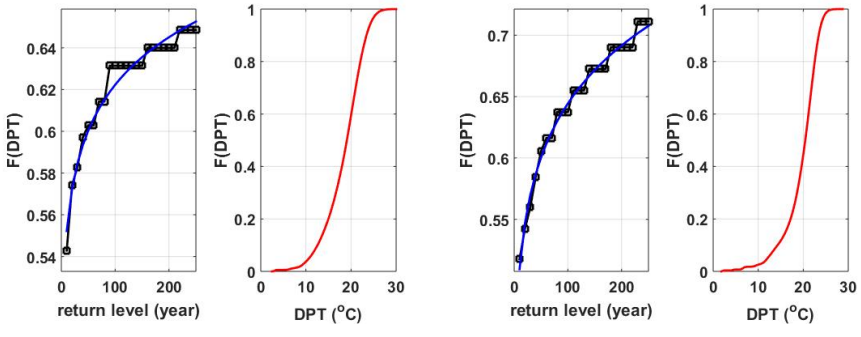

838

839

Figure 6. Selection of reference dew-point temperature for estimating rainfall quantiles at (a) Busan and (b) Seoul sites. In this figure, 'F(DPT)' refers to the empirical cumulative probabilities of DPT on the day of POT excess.

843

https://doi.org/10.5194/hess-2020-167
Preprint. Discussion started: 12 May 2020

Hydrology and Earth System Sciences
Discussions

844

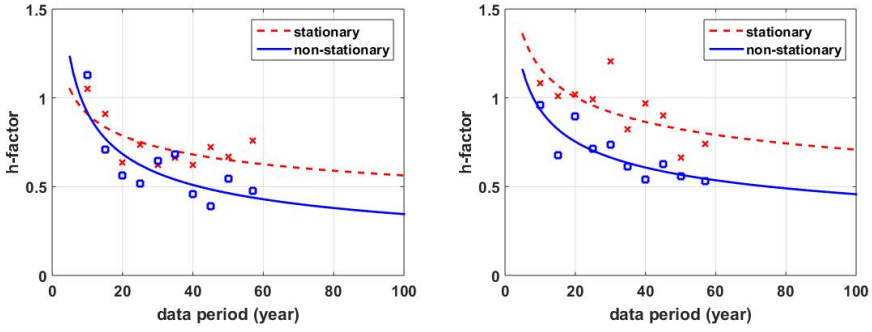

845

846 **(a) Busan** **(b) Seoul**

847 **Figure 7. Effect of the number of samples on the uncertainty of rainfall quantile using reference dew-point**
848 **temperature.**

849

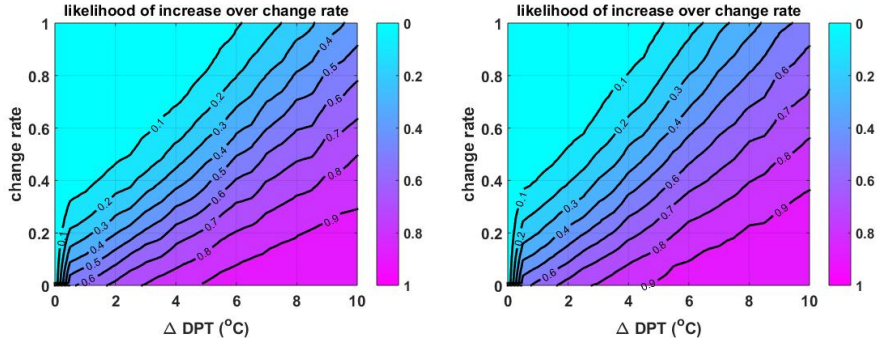

850

851 **(a) Busan** **(b) Seoul**

852 **Figure 8. Likelihood of increase over change rate of rainfall quantile for return level of 100-year.**

853

854

https://doi.org/10.5194/hess-2020-167
Preprint. Discussion started: 12 May 2020

Hydrology and Earth System Sciences
Discussions
Open Access
EGU

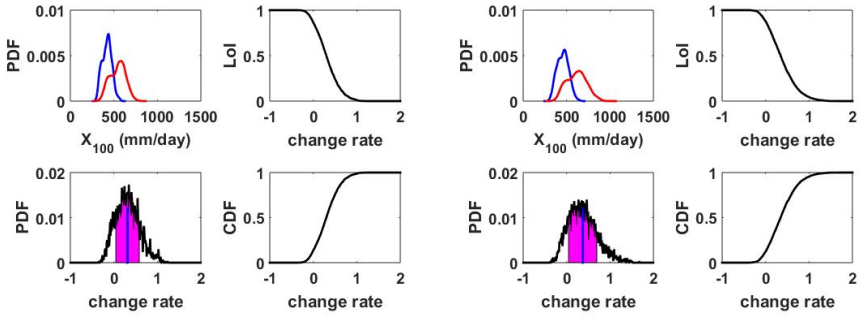

855

856 **(a) Busan** **(b) Seoul**

857 **Figure 9. Procedure for analyzing uncertainty in rate of change. In upper left figures, the blue line is the**
858 **probability distribution of X_p^T in the present condition, and the red line is the probability distribution of**
859 **X_f^T in the DPT 4 ℃ rising condition. In the lower left figures, the section of the standard deviation was**
860 **colored in pink.**

861

862